10 Jul 2020

Collective Modes at a Disordered Quantum Phase Transition

Martin Puschmann

Jack Crewse

Jose A. Hoyos

Thomas Vojta
Missouri University of Science and Technology, vojtat@mst.edu

Recommended Citation

M. Puschmann et al., "Collective Modes at a Disordered Quantum Phase Transition," *Physical Review Letters*, vol. 125, no. 2, American Physical Society (APS), Jul 2020.
The definitive version is available at https://doi.org/10.1103/PhysRevLett.125.027002

Collective Modes at a Disordered Quantum Phase Transition

Martin Puschmann,[1] Jack Crewse,[1] José A. Hoyos,[2] and Thomas Vojta[1]
[1]Department of Physics, Missouri University of Science and Technology, Rolla, Missouri 65409, USA
[2]Instituto de Física de São Carlos, Universidade de São Paulo, C.P. 369, São Carlos, São Paulo 13560-970, Brazil

(Received 21 November 2019; accepted 23 June 2020; published 10 July 2020)

We study the collective excitations, i.e., the Goldstone (phase) mode and the Higgs (amplitude) mode, near the superfluid–Mott glass quantum phase transition in a two-dimensional system of disordered bosons. Using Monte Carlo simulations as well as an inhomogeneous quantum mean-field theory with Gaussian fluctuations, we show that the Higgs mode is strongly localized for all energies, leading to a noncritical scalar response. In contrast, the lowest-energy Goldstone mode undergoes a striking delocalization transition as the system enters the superfluid phase. We discuss the generality of these findings and experimental consequences, and we point out potential relations to many-body localization.

DOI: 10.1103/PhysRevLett.125.027002

Understanding the rich behavior that arises when many quantum particles interact with each other remains one of the major challenges of modern condensed matter physics. Zero-temperature phase transitions between different quantum ground states have emerged as a central ordering principle in this field [1–6]. These quantum phase transitions (QPTs) control large regions of a material's phase diagram and lead to unconventional thermodynamic and transport properties. Moreover, fluctuations associated with these transitions can induce novel phases, increasing the complexity of quantum matter.

Since impurities, defects, and other types of quenched disorder are unavoidable in most condensed matter systems, the effects of randomness on QPTs have been studied intensively over the last two decades, leading to the discovery of exotic phenomena such as infinite-randomness critical points [7], smeared phase transitions [8], and quantum Griffiths singularities [9]. Today, the thermodynamics of many disordered QPTs is well understood, and classification schemes [10,11] have been established based on the scaling of the disorder strength under coarse graining as well as on the importance of rare disorder fluctuations (see, e.g., Ref. [12] and references therein).

Much less is known about the character and dynamics of excitations at disordered QPTs even though excitations are crucial for a host of experiments ranging from inelastic neutron scattering in magnetic materials to various electrical and thermal transport measurements. Of particular interest are the collective excitations that emerge in systems with spontaneously broken continuous symmetries. These include one or more Goldstone modes that are related to oscillations of the order parameter direction and an amplitude (Higgs) mode that is related to oscillations of the order parameter magnitude. Examples of such modes can be found in superfluids, superconductors, incommensurate charge density waves, as well as planar and Heisenberg magnets (see, e.g., Refs. [13,14]).

In this Letter, we therefore investigate the excitations close to a paradigmatic disordered QPT, the superfluid-Mott glass transition of disordered bosons, by means of Monte Carlo simulations and an inhomogeneous mean-field theory with Gaussian fluctuations. Our results can be summarized as follows. Even though the thermodynamic critical behavior of the superfluid-Mott glass transition is of conventional power-law type [15,16], the Higgs and Goldstone modes feature unconventional dynamics that violates naive scaling. Specifically, the Higgs mode is strongly localized, resulting in a broad, noncritical spectral density close to the QPT. In contrast, the incipient Goldstone mode features a striking delocalization transition as the system enters the superfluid phase, irrespective of the disorder strength.

In the remainder of this Letter, we first introduce our model and then discuss the Monte Carlo simulations. To explain the unusual, noncritical response observed in these simulations, we study Gaussian fluctuations about an inhomogeneous quantum mean-field theory. We also discuss possible experiments, and consider relations to many-body localization.

We start from a square-lattice Bose-Hubbard Hamiltonian

$$H = \frac{1}{2}\sum_i U_i(n_i - \bar{n})^2 - \sum_{\langle ij\rangle} J_{ij}(a_i^\dagger a_j + \text{H.c.}) \quad (1)$$

with large integer filling $\bar{n}$. Here, $a_i^\dagger$ and a are the boson creation and annihilation operators at site i, and $n_i = a_i^\dagger a_i$ is the number operator. If the interactions U_i and the nearest-neighbor hopping terms J_{ij} are spatially uniform,

the system undergoes a QPT between a superfluid ground state (for $J \gg U$) and a gapped, incompressible Mott insulator (for $J \ll U$). In the presence of quenched disorder, these two bulk phases are separated by the Mott glass phase, a gapless but incompressible insulator [17,18]. In the following, we introduce the disorder via site dilution, i.e., we randomly remove a nonzero fraction p of lattice sites while the U_i and J_{ij} of the remaining sites stay uniform.

To study the collective modes across the superfluid-Mott glass transition, we map the Bose-Hubbard model (1) onto a $(2+1)$-dimensional XY model [19] with columnar defects. We then perform large-scale Monte Carlo simulations for lattices with linear sizes of up to $L = 256$ and $L_\tau = 512$ in the space and imaginary time directions. The phase diagram and the thermodynamic critical behavior (which is of conventional power-law type) are known accurately from earlier studies [16,20]. For details of the simulations and the data analysis see the Supplemental Material [21].

To analyze the Higgs mode, we compute the (disorder-averaged) imaginary-time scalar susceptibility,

$$\chi_{\rho\rho}(\mathbf{x},\tau) = \langle \rho(\mathbf{x},\tau)\rho(0,0)\rangle - \langle \rho(\mathbf{x},\tau)\rangle\langle \rho(0,0)\rangle \quad (2)$$

and its Fourier transform $\tilde{\chi}_{\rho\rho}(\mathbf{q}, i\omega_m)$. Here, $\rho(\mathbf{x},\tau)$ is the local order parameter amplitude, obtained as the average of the XY variables over a small (five-site) cluster. The dynamic susceptibility is given by the analytic continuation from imaginary Matsubara frequencies $i\omega_m$ to real frequencies ω,

$$\chi_{\rho\rho}(\mathbf{q},\omega) = \tilde{\chi}_{\rho\rho}(\mathbf{q}, i\omega_m \to \omega + i0^+). \quad (3)$$

Unfortunately, the analytic continuation is an ill-posed problem and sensitive to Monte Carlo noise. To overcome this problem, we employ a maximum-entropy (MaxEnt) method [34]. Its technical details and robustness are discussed in the Supplemental Material [21]. Generalizing scaling arguments of Podolsky and Sachdev [35] to the disordered case suggests that the singular part of the scalar susceptibility in d space dimensions has the form

$$\chi_{\rho\rho}(\mathbf{q},\omega) = \omega^{[(d+z)\nu-2]/(\nu z)} X(\mathbf{q}r^{-\nu}, \omega r^{-\nu z}), \quad (4)$$

where r is the distance from criticality, ν is the correlation length exponent, z is the dynamical exponent, and X is a universal scaling function [21].

We now turn to the results of the Monte Carlo simulations. Figure 1 shows the spectral function $\chi''_{\rho\rho}(\mathbf{q},\omega)$ at $\mathbf{q} = 0$ on superfluid side of the QPT, contrasting the clean case ($p = 0$) with a diluted case ($p = 1/3$). The clean spectral function features a pronounced low-energy Higgs peak that softens as the transition is approached. The low-energy part of $\chi''_{\rho\rho}$ fulfills the scaling form (4) in good

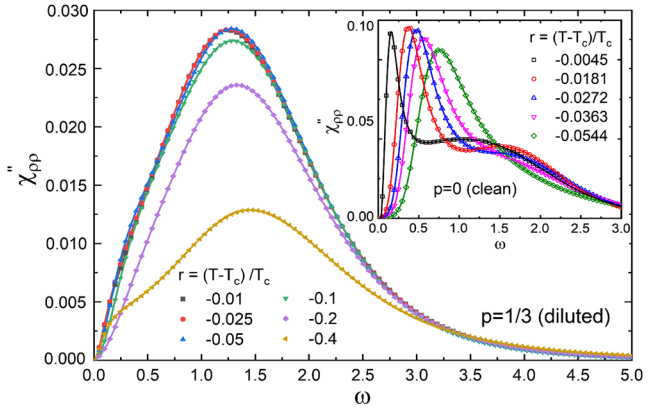

FIG. 1. Spectral function $\chi''_{\rho\rho}(\mathbf{q}=0,\omega)$ for different distances r from criticality on the superfluid side of the transition. Main panel: dilution $p = 1/3$, results averaged over 10 000 samples of sizes $L = 100$, $L_\tau = 452$. Inset: clean case ($p = 0$), $L = L_\tau = 128$. Statistical errors are small, about one symbol size; variations of the MaxEnt parameters can shift the peak positions systematically by up to about 10% [21]. T is the Monte Carlo temperature, not the physical temperature of the Bose-Hubbard Hamiltonian.

approximation, using the exponents $\nu = 0.671$ and $z = 1$ of the clean 3D XY universality class [36] (see Fig. S1 in the Supplemental Material [21]). These findings agree with previous simulations of the Higgs mode at the clean superfluid-Mott insulator transition [37,38].

The spectral function of the diluted system behaves very differently. Instead of a narrow low-energy peak, it features a broad maximum at higher energies. Importantly, the position of this maximum is only weakly dependent on the distance r from criticality; it does not vanish for $r \to 0$. This behavior violates the scaling form (4), implying that the scalar susceptibility is dominated by a noncritical contribution.

We also study the dispersion $\omega_H(\mathbf{q})$ of the peak position as a function of the wave vector $\mathbf{q}$; the results are presented in Fig. 2. In the clean case, the data show the behavior expected for a $z = 1$ quantum critical point. The low-energy dispersion is linear, $\omega_H \sim |\mathbf{q}|$, at criticality. As r increases, it crosses over to the quadratic form $\omega_H = m_H + c\mathbf{q}^2$. In contrast, the dispersion of the diluted system does not change much with the distance from criticality, and the peak energy ω_H is almost independent of $\mathbf{q}$ for small wave vectors.

What causes the broad, uncritical scalar response near the superfluid-Mott glass transition? Potential reasons include increased damping and localization effects. To gain further insight and to disentangle these possibilities, we complement the Monte Carlo simulations by an inhomogeneous mean-field theory with Gaussian fluctuations. Our approach generalizes the theories of Refs. [39,40] to the disordered case. It is also related to the bond-operator method for disordered magnets [41].

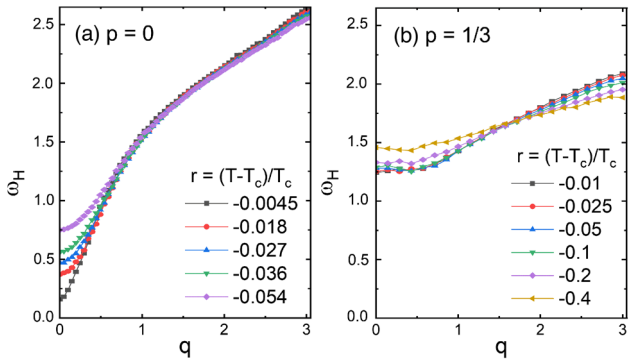

FIG. 2. Peak position ω_H of the spectral function $\chi''_{\rho\rho}(\mathbf{q},\omega)$ vs wave vector $|\mathbf{q}|$ (along the coordinate directions) for different distances r from criticality. (a) dilution $p=0$. (b) $p=1/3$. The simulation parameters agree with Fig. 1. Statistical errors are about a symbol size or less.

Close to the Mott phase, particle number fluctuations are small. We thus truncate the local Hilbert space at site j to three basis states, $|-_j\rangle, |0_j\rangle$, and $|+_j\rangle$, corresponding to the boson numbers $n_j=\bar{n}-1,\bar{n}$, and $\bar{n}+1$, respectively. The mean-field theory derives from the variational ground state wave function $|\Phi_0\rangle=\prod_j|\phi_{0j}\rangle$ with

$$|\phi_{0j}\rangle=\cos(\theta_j/2)|0_j\rangle + \sin(\theta_j/2)(e^{i\eta_j}|+_j\rangle+e^{-i\eta_j}|-_j\rangle)/\sqrt{2}. \quad (5)$$

It captures both the Mott state, $\theta_j=0$, and the superfluid state, $\theta_j>0$, with the local superfluid order parameter $\langle a_j^\dagger\rangle\propto\psi_j=\sin\theta_j e^{-i\eta_j}$.

The variational ground state energy $E_0=\langle\Phi_0|H|\Phi_0\rangle$ is minimized by uniform phases $\eta_j=\eta=\text{const}$ (which we set to zero in the following) and mixing angles θ_i that fulfill the mean-field equations

$$U_i\sin\theta_i-4\bar{n}\cos\theta_i\sum_j J_{ij}\sin\theta_j=0. \quad (6)$$

To describe excitations on top of the mean-field ground state, we rotate the basis in the three-state local Hilbert space of site j to $|\phi_{0j}\rangle,|\phi_{Hj}\rangle,|\phi_{Gj}\rangle$ where

$$|\phi_{Hj}\rangle=\sin(\theta_j/2)|0_j\rangle-\cos(\theta_j/2)(|+_j\rangle+|-_j\rangle)/\sqrt{2},$$
$$|\phi_{Gj}\rangle=i(|+_j\rangle-|-_j\rangle)/\sqrt{2} \quad (7)$$

are related to changes of order parameter magnitude and phase, respectively, compared to $|\phi_{0j}\rangle$. The boson operators $b_{0j}^\dagger, b_{Hj}^\dagger$, and $b_{Gj}^\dagger$ create these states out of the fictitious vacuum and fulfill the local constraint $\sum_\alpha b_{\alpha j}^\dagger b_{\alpha j}=1$. We now rewrite the Hamiltonian (1) in terms of the b bosons, using the constraint to eliminate ("fully condense") b_{0j} such that $b_{Hj}^\dagger$ and $b_{Gj}^\dagger$ create excitations on top of the mean-field ground state. To quadratic (Gaussian) order in b, the Hamiltonian decouples into Higgs and Goldstone parts, $H=E_0+H_H+H_G$, which both take the form

$$H_\alpha=\sum_i A_{\alpha i}b_{\alpha i}^\dagger b_{\alpha i}+\sum_{\langle ij\rangle}B_{\alpha ij}(b_{\alpha i}^\dagger+b_{\alpha i})(b_{\alpha j}^\dagger+b_{\alpha j}), \quad (8)$$

($\alpha=H,G$). The coefficients $A_{\alpha i}$ and $B_{\alpha ij}$ are nonuniform and depend on the mixing angles θ_i. H_H and H_G can be diagonalized numerically by bosonic Bogoliubov transformations, $b_{\alpha j}=\sum_k(u_{\alpha jk}d_{\alpha k}+v_{\alpha jk}^*d_{\alpha k}^\dagger)$ [21].

We now present the results of the mean-field theory. In the absence of dilution, $p=0$, the mean-field equation (6) can be solved analytically. A superfluid solution appears for $U<U_c^0=4\bar{n}Jz$ where $z=4$ is the coordination number of the lattice; it has a uniform mixing angle $\cos\theta=U/U_c^0$ and order parameter $\psi=(1-U/U_c^0)^{1/2}$. As the system is translationally invariant, all excitations have plane wave character. In the superfluid phase, the Goldstone mode is gapless while the gapped Higgs mode softens at the QPT. In the insulating phase the two modes are gapped and degenerate. All clean mean-field results agree with earlier work [39].

The behavior changes dramatically in the presence of disorder. Figure 3 shows the average and typical order parameter for site dilutions $p=1/8$ and $1/3$, resulting from a numerical solution of the mean-field equations (6) [42]. As expected, the onset of superfluidity is suppressed compared to the clean case, $p=0$. The large difference between the average and typical order parameter for $U/(\bar{n}J)$ slightly below the onset of superfluidity indicates the coexistence of superfluid puddles with insulating regions, characteristic of a Griffiths phase (which is wider for stronger dilution). At lower U, the order parameter is only moderately inhomogeneous.

Turning to excitations on top of the mean-field ground state, Fig. 4(a) visualizes examples of the lowest-energy

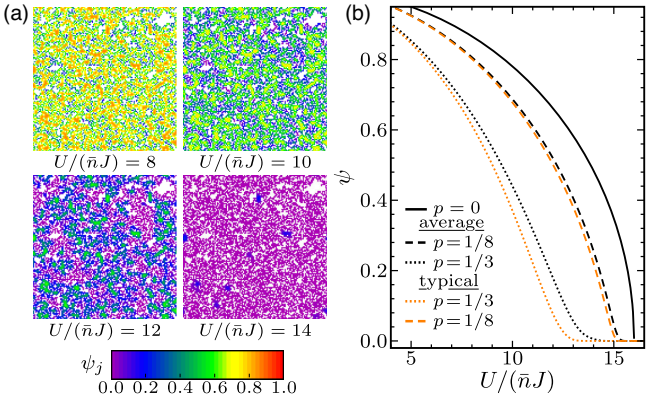

FIG. 3. (a) Local order parameter ψ_j for several $U/(\bar{n}J)$ for a system of 128^2 sites with dilution $p=1/3$. (b) Average and typical (geometric average) local order parameter ψ as function of $U/(\bar{n}J)$ for dilutions $p=0,1/8$, and $1/3$, using 1000 disorder realizations. Statistical errors are comparable to the linewidths.

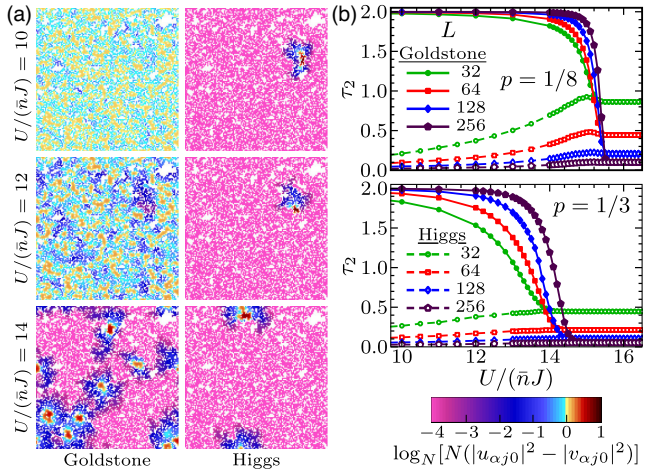

FIG. 4. (a) Wave functions of the lowest-energy Goldstone and Higgs modes for $p = 1/3$ and several $U/(\bar{n}J)$, visualized as $|u_{\alpha j0}|^2 - |v_{\alpha j0}|^2$. (b) Generalized dimension τ_2 of the lowest-energy Goldstone and Higgs modes vs interaction $U/(\bar{n}J)$ for $p = 1/8$ and $1/3$ (averaged over 1000 disorder realizations). Statistical errors are smaller than the symbol size.

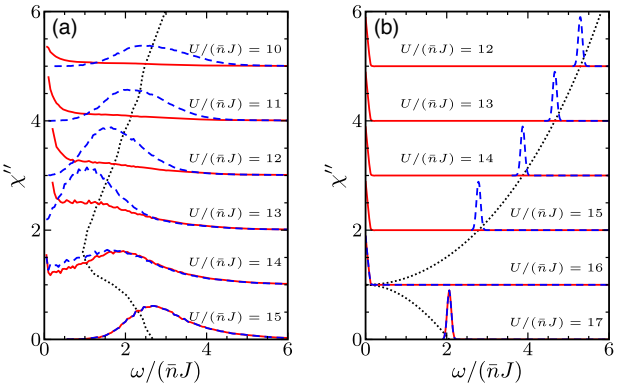

FIG. 5. Spectral functions $\chi''(\mathbf{q} = 0, \omega)$ of the Goldstone (solid lines) Higgs (dashed lines) excitations for several interactions $U/(\bar{n}J)$. The curves are shifted upward with increasing U. Dotted lines mark the position of the Higgs peak in χ''. (a) Dilution $p = 1/3$ (240 disorder realizations, statistical errors are comparable to the linewidths). (b) Clean case, $p = 0$; here the peaks in the figure represent δ functions.

eigenstates in both the Higgs and Goldstone channels for dilution $p = 1/3$. Clearly, these states show nontrivial localization properties. To characterize the localization, we calculate the inverse participation number $P^{-1}(0) = \sum_j (|u_{\alpha j0}|^2 - |v_{\alpha j0}|^2)^2$ [41] and the corresponding generalized dimension $\tau_2(0) = \ln P(0)/\ln L$ [43]. The dependence of τ_2 on the interaction U for the lowest-energy eigenstates in the Higgs and Goldstone channels is presented in Fig. 4(b). For both weak and strong dilutions, $p = 1/8$ and $1/3$, we observe the same behavior. In the insulating phase, both excitations are degenerate and strongly localized as indicated by the rapid drop of τ_2 toward zero with increasing L.

Upon entering the superfluid phase with decreasing U, the two excitations evolve in opposite directions. The Higgs mode becomes even more localized, reflected in a further decrease of τ_2. In contrast, the lowest Goldstone excitation undergoes a rapid delocalization transition. Its dimension τ_2 increases quickly, and its L dependence changes sign. It now increases toward $\tau_2 = 2$ with increasing L, indicating an extended state. Within our numerical accuracy, the crossing of the τ_2 vs $U/(\bar{n}J)$ curves coincides with the onset of superfluid order. In fact, we have derived an analytic expression for the wave function of the lowest Goldstone excitation in the superfluid phase that proves that it is extended whenever the system features a macroscopic order parameter [21].

We also study the dependence of the localization on the excitation energy [21]. On the insulating side, the excitations are strongly localized for all energies, and the same is true for the Higgs mode in the superfluid phase. Goldstone excitations with nonzero energy appear to be localized as well, with a localization length that diverges with vanishing energy. We do not find any evidence for a mobility edge at nonzero energy, in contrast to the Bose glass results reported in Ref. [44].

To establish a connection to the Monte Carlo simulations, we compute the spectral densities of the Higgs and Goldstone Green functions $\chi_{\alpha jk}(t) = -i\Theta(t)\langle[b^\dagger_{\alpha j}(t) + b_{\alpha j}(t), b^\dagger_{\alpha k}(0) + b_{\alpha k}(0)]\rangle$ with $\alpha = G, H$. Figure 5 shows the spectral densities at zero wave vector for several interactions $U/(\bar{n}J)$, comparing the clean case with dilution $p = 1/3$. The spectral densities of the diluted system are very broad, even though the eigenmodes are noninteracting within the Gaussian approximation and thus have no intrinsic width. This demonstrates that the broadening of χ'' is due to disorder-induced localization effects. Moreover, the peak in the Higgs spectral function does not soften at the superfluid-Mott glass transition, mirroring the Monte Carlo results in Fig. 1. In contrast, the clean spectral functions show the expected δ peaks at energies corresponding to the Higgs and Goldstone masses.

To summarize, we found the Higgs mode to be strongly localized across the superfluid-Mott glass QPT; the scalar response is thus noncritical and violates naive scaling. The lowest Goldstone excitation, in contrast, delocalizes upon entering the superfluid phase. Higher-energy Goldstone excitations are localized, implying the absence of a nonzero-energy mobility edge for the excitations.

The mean-field theory used in the second half of this Letter provides only an approximate description of the superfluid-Mott glass transition. In particular, it does not correctly capture rare regions effects because it cannot describe the fluctuations of large superfluid puddles in an insulating matrix. Whereas rare regions are known to be unimportant for the thermodynamics of this QPT [12], their effects on excitations are less well understood. Moreover, the Gaussian approximation for H_H and H_G neglects

anharmonic effects (which could be included by keeping higher-order terms in the expansion of H). However, the agreement between the mean-field results and the numerically exact Monte Carlo simulations gives us confidence in their validity.

Potential routes to analyze the superfluid-Mott glass transition experimentally include ultracold atoms, dirty and granular superconductors, as well as diluted quantum antiferromagnets. Recently, the effects of the Higgs mode on the dynamical conductivity in disordered superconducting thin films were modeled by a bosonic Hamiltonian similar to ours [45,46]. The Monte Carlo data in these papers appear to be compatible with a more conventional scenario in which the Higgs response sharpens and softens as the QPT is approached. We believe that this may stem from the comparatively weak disorder used in Refs. [45,46] which causes a slow crossover to the disordered behavior [47].

In conclusion, our work demonstrates that disordered QPTs can feature unconventional collective excitations even if their thermodynamic critical behavior is completely regular. This implies a number of important general questions about collective modes at disordered QPTs: Can one classify the excitation dynamics along similar lines as the thermodynamics? What is the character (and critical behavior) of the delocalization transition of the Goldstone mode? Under what conditions does a mobility edge appear? Is it related to many-body localization? What role is played by the space dimensionality? These questions remain tasks for the future.

This work was supported by the NSF under Grants No. DMR-1506152, No. DMR-1828489, No. PHY-1125915, and No. PHY-1607611, by Conselho Nacional de Desenvolvimento Científico e Tecnológico (CNPq) under Grant No. 312352/2018-2, and by FAPESP under Grants No. 2015/23849-7 and No. 2016/10826-1. T. V. and J. A. H. acknowledge the hospitality of the Aspen Center for Physics, and T. V. thanks the Kavli Institute for Theoretical Physics where part of the work was performed.

[1] S. Sachdev, *Quantum Phase Transitions* (Cambridge University Press, Cambridge, England, 2011).
[2] S. L. Sondhi, S. M. Girvin, J. P. Carini, and D. Shahar, Rev. Mod. Phys. **69**, 315 (1997).
[3] T. Vojta, Ann. Phys. (Leipzig) **9**, 403 (2000).
[4] M. Vojta, Rep. Prog. Phys. **66**, 2069 (2003).
[5] H. v. Löhneysen, A. Rosch, M. Vojta, and P. Wölfle, Rev. Mod. Phys. **79**, 1015 (2007).
[6] Q. Si and F. Steglich, Science **329**, 1161 (2010).
[7] D. S. Fisher, Phys. Rev. Lett. **69**, 534 (1992); Phys. Rev. B **51**, 6411 (1995).
[8] T. Vojta, Phys. Rev. Lett. **90**, 107202 (2003); J. A. Hoyos and T. Vojta, Phys. Rev. Lett. **100**, 240601 (2008).
[9] M. Thill and D. A. Huse, Physica (Amsterdam) **214A**, 321 (1995); H. Rieger and A. P. Young, Phys. Rev. B **54**, 3328 (1996).
[10] O. Motrunich, S. C. Mau, D. A. Huse, and D. S. Fisher, Phys. Rev. B **61**, 1160 (2000).
[11] T. Vojta and J. Schmalian, Phys. Rev. B **72**, 045438 (2005); T. Vojta and J. A. Hoyos, Phys. Rev. Lett. **112**, 075702 (2014).
[12] T. Vojta, J. Phys. A **39**, R143 (2006); J. Low Temp. Phys. **161**, 299 (2010); Annu. Rev. Condens. Matter Phys. **10**, 233 (2019).
[13] C. Burgess, Phys. Rep. **330**, 193 (2000).
[14] D. Pekker and C. Varma, Annu. Rev. Condens. Matter Phys. **6**, 269 (2015).
[15] N. Prokof'ev and B. Svistunov, Phys. Rev. Lett. **92**, 015703 (2004).
[16] T. Vojta, J. Crewse, M. Puschmann, D. Arovas, and Y. Kiselev, Phys. Rev. B **94**, 134501 (2016).
[17] T. Giamarchi, P. Le Doussal, and E. Orignac, Phys. Rev. B **64**, 245119 (2001).
[18] P. B. Weichman and R. Mukhopadhyay, Phys. Rev. B **77**, 214516 (2008).
[19] M. Wallin, E. S. Sørensen, S. M. Girvin, and A. P. Young, Phys. Rev. B **49**, 12115 (1994).
[20] C. Lerch and T. Vojta, Eur. Phys. J. Special Topics **227**, 2275 (2019).
[21] See Supplemental Material at http://link.aps.org/supplemental/10.1103/PhysRevLett.125.027002, which includes Refs. [22–33], for details of the Monte Carlo simulations, the scaling form of the scalar susceptibility, the maximum-entropy method, and the quantum mean-field theory.
[22] U. Wolff, Phys. Rev. Lett. **62**, 361 (1989).
[23] N. Metropolis, A. W. Rosenbluth, M. N. Rosenbluth, A. H. Teller, and E. Teller, J. Chem. Phys. **21**, 1087 (1953).
[24] M. Guo, R. N. Bhatt, and D. A. Huse, Phys. Rev. Lett. **72**, 4137 (1994).
[25] H. Rieger and A. P. Young, Phys. Rev. Lett. **72**, 4141 (1994).
[26] R. Sknepnek, T. Vojta, and M. Vojta, Phys. Rev. Lett. **93**, 097201 (2004); T. Vojta and R. Sknepnek, Phys. Rev. B **74**, 094415 (2006).
[27] H. G. Ballesteros, L. A. Fernández, V. Martín-Mayor, A. Muñoz Sudupe, G. Parisi, and J. J. Ruiz-Lorenzo, Phys. Rev. B **58**, 2740 (1998).
[28] Q. Zhu, X. Wan, R. Narayanan, J. A. Hoyos, and T. Vojta, Phys. Rev. B **91**, 224201 (2015).
[29] J. T. Chayes, L. Chayes, D. S. Fisher, and T. Spencer, Phys. Rev. Lett. **57**, 2999 (1986).
[30] P. Hansen and D. O'leary, SIAM J. Sci. Comput. **14**, 1487 (1993).
[31] D. Bergeron and A.-M. S. Tremblay, Phys. Rev. E **94**, 023303 (2016).
[32] A. MacKinnon and B. Kramer, Z. Phys. B **53**, 1 (1983).
[33] A. MacKinnon, Z. Phys. B **59**, 385 (1985).
[34] M. Jarrell and J. Gubernatis, Phys. Rep. **269**, 133 (1996).
[35] D. Podolsky and S. Sachdev, Phys. Rev. B **86**, 054508 (2012).
[36] M. Campostrini, M. Hasenbusch, A. Pelissetto, and E. Vicari, Phys. Rev. B **74**, 144506 (2006).

[37] S. Gazit, D. Podolsky, and A. Auerbach, Phys. Rev. Lett. **110**, 140401 (2013).
[38] K. Chen, L. Liu, Y. Deng, L. Pollet, and N. Prokof'ev, Phys. Rev. Lett. **110**, 170403 (2013).
[39] E. Altman and A. Auerbach, Phys. Rev. Lett. **89**, 250404 (2002).
[40] D. Pekker, B. Wunsch, T. Kitagawa, E. Manousakis, A. S. Sørensen, and E. Demler, Phys. Rev. B **86**, 144527 (2012).
[41] M. Vojta, Phys. Rev. Lett. **111**, 097202 (2013).
[42] For each lattice, we only consider the infinite percolation cluster as finite clusters cannot support superfluid long-range order.
[43] In our numerical calculations, we compute τ_2 via the box-counting method, see the Supplemental Material, Ref. [21].
[44] J. P. Álvarez Zúñiga and N. Laflorencie, Phys. Rev. Lett. **111**, 160403 (2013).
[45] M. Swanson, Y. L. Loh, M. Randeria, and N. Trivedi, Phys. Rev. X **4**, 021007 (2014).
[46] D. Sherman, U. S. Pracht, B. Gorshunov, S. Poran, J. Jesudasan, M. Chand, P. Raychaudhuri, M. Swanson, N. Trivedi, A. Auerbach, M. Scheffler, A. Frydman, and M. Dressel, Nat. Phys. **11**, 188 (2015).
[47] This is supported by the fact that the critical behavior found in Ref. [45] agreed with a clean dynamical exponent $z = 1$ rather than the disordered value $z = 1.52$ [16].